Calibration and evaluation of the STICS soil-crop model for faba bean to explain variability in yield and N2 fixation

Gatien Falconnier, Etienne-Pascal Journet, Laurent Bedoussac, Anthony Vermue, Florent Chlebowski, Nicolas Beaudoin, Eric Justes

Calibration and evaluation of the *STICS* soil-crop model for faba bean to explain variability in yield and N_2 fixation

Gatien N. Falconnier[1,5], Etienne-Pascal Journet[1,2], Laurent Bedoussac[3], Anthony Vermue[1], Florent Chlébowski[4], Nicolas Beaudoin[4], Eric Justes[1,6]

[1] AGIR, Université de Toulouse, INPT, INP-PURPAN, INRA, 31320, Auzeville, France

[2] LIPM, Université de Toulouse, INRA, CNRS, Castanet-Tolosan, France

[3] AGIR, Université de Toulouse, INPT, INP-PURPAN, INRA, ENSFEA, 31320, Auzeville, France

[4]UR INRA 1158 Agro-Impact, site de Laon, Pôle du Griffon, F-02000 Barenton-Bugny.

[5] Current affiliation: CIRAD, UPR-Agro-Ecology and Sustainable Intensification of Annual Crops, University of Montpellier, Avenue Agropolis, 34398 Montpellier France

[6] Current affiliation: CIRAD, UMR SYSTEM, Montpellier Univ, CIHEAM-IAMM, CIRAD, INRA, Montpellier SupAgro, 2 place Viala, F-34060 Montpellier

Abstract:

Faba bean (*Vicia Faba* L.) is the second most widely grown grain legume in Europe after pea (*Pisum Sativum* L.) and presents several agronomic and environmental advantages when inserted in cropping systems (*e.g.* decreased dependency on synthetic fertilisers and N provision to the subsequent crop). However, yield variability due to several factors including heat and drought impede wide adoption of faba bean by farmers. Soil-crop models provide quantitative information to evaluate these processes and help to design innovative cropping system including legumes. The *STICS* model was chosen for its agro-environmental purpose

and its genericity allowing crop rotation simulation and robustness for a wide range of pedoclimatic conditions. However, there is so far for *STICS* no parameterization for faba bean. We calibrated 38 crop related parameters based on literature, direct measurements and sequential estimation using the optimisation tool *OptimiSTICS* and a dataset of winter faba bean grown in two sites in France with contrasting soil conditions over several growing seasons (2002-2015). Data from 22 experimental plots were used for calibration and the remaining independent 13 plots were used for model evaluation. After calibration, the *STICS* model reproduced well phenology, Leaf Area Index and dynamic growth of above ground biomass, uptake of mineral N, N_2 fixation and grain yield, with satisfactory model efficiency (0.56 to 0.81) and low relative bias (-7% to 2%). The model adequately reproduced the large observed variation in faba bean grain yield (0.42 – 4.70 t ha^{-1}) and total N_2 fixed at harvest (62 – 172 kg N ha^{-1}) in the contrasted years and soil conditions of this study. Simulations indicated that water stress was the overriding factor driving yield and N_2 fixation variability. Simulation of temporal crop growth and water stresses during grain onset and grain filling allowed a robust and credible agronomic diagnosis of the causes of this variability for faba bean crops not significantly damaged by pests and diseases. Water supply/demand ratio averaged over a period of six days preceding beginning of grain filling explained 78% of the observed grain yield variability while water deficit factor for N_2 fixation averaged over a period of 20 days following the beginning of grain filling explained 83% of the variability of fixed N_2 at harvest. Our work provides a first calibration and evaluation of the *STICS* model for faba bean. It offers the opportunity to quantify the ecosystem services associated with crop rotations including faba bean and the effect of climate change on the performance of such rotations.

Keywords: *parameter estimation, yield variability, abiotic stresses, grain legume*

1. Introduction

Current cropping systems in Europe are characterized by high productivity but rely on simplification of crop rotations and high level of synthetic inputs which has led to soil, water and air pollution and loss of biodiversity (*e.g.* Stoate et al. 2009). Diversification of current cropping systems with grain legumes can improve agronomic, economic and environmental performance and provide supporting and regulating ecosystem services. In particular, relying on biological N_2 fixation decreases the dependence on synthetic nitrogen fertilizer and reduces the associated direct and indirect greenhouse gases emissions and risks of nitrate leaching (Plaza-Bonilla et al., 2017; Reckling et al., 2016). However, legumes often suffer from water and temperature stress: i) drought during reproductive phase can cause severe yield reduction (Daryanto et al., 2017) and ii) heat can impact negatively seed set and grain filling (Prasad et al., 2017). Even though not always well appreciated, N_2 fixation can also be severely restricted by stresses due to drought, heat, anoxia and soil mineral N content in the root zone (Liu et al., 2011). Furthermore, legumes are exposed to damages from pests, diseases and weeds at different time in their growth cycle (Rubiales et al., 2015). Strong yield variability and lack of reliable agronomic diagnosis are the main reasons mentioned by farmers for non-adoption of legumes in cropping systems (Meynard et al., 2017; Watson et al., 2017). Dynamic process based soil crop models can assist the understanding of current yield variability by simulating patterns of seasonal water and temperature stress (Affholder et al., 2003; Hayman et al., 2010). They are useful tools to diagnose agronomic constraints to crop production and to explore the impact of current and future climate variability. Therefore, they can assist the design of more resilient cropping systems by analysing model outputs. Furthermore, these models allow to estimate indicators that are crucial for the assessment of crop rotations but tedious or expensive to quantify in experimental plots, *e.g.* biological N_2

fixation (Liu et al., 2011), water drainage (Bruelle et al., 2017), N_2O emissions or nitrate leaching (Plaza-Bonilla et al., 2015).

The *STICS* model is a generic dynamic soil-crop model that has been used to assess the agronomic and environmental performances of crop rotations and to support the design of innovative cropping systems in a wide range of agro-pedo-climatic conditions (Coucheney et al., 2015). For example, Bécel et al. (2015) assessed the impact of various integrated weed management strategies on nitrate leaching. Constantin et al. (2015) determined the optimal date of emergence and destruction of cover crops to reduce nitrate leaching. Jégo et al. (2010) analyzed the effect of fertilization, irrigation strategies and climate variability on nitrate leaching in sugar beet/potato cropping systems. So far, spring pea (*Pisum Sativum* L.) and soybean (*Glycine max* (L.) Merr.) are the only grain legume calibrated for *STICS* (Corre-Hellou et al., 2009; Jégo et al., 2010). *STICS* can simulate N sharing between companion crops and N carry over effects on following crops, but all the involved crops must be calibrated for *STICS*. Given the potential of grain legume to improve cropping system sustainability in Europe (Watson et al., 2017) and the potential of crop models to help with the design of innovative and resilient cropping systems including legumes, there is a need to broaden the number of grain legume crops calibrated and evaluated with the *STICS* cropping system model.

Faba bean (*Vicia Faba* L.) is the second most widely grown European grain legumes (Watson et al., 2017). Its proportion of crop N derived from atmospheric N_2 is the greatest among major grain legumes cultivated in Europe (153 kg N ha^{-1} on average) (Jensen et al. 2010). It is a high-biomass crop leaving more residues and giving a greater nitrogen-related yield effect on the subsequent crop compared with low biomass crop like chickpea and lentil for example (Watson et al., 2017). However faba bean, like other legume crops, can suffer from strong

yield and N_2 fixation reduction due to abiotic factors (Bishop et al., 2016; Khan et al., 2010; López-Bellido et al., 2011) and pests and diseases (Stoddard et al., 2010).

Winter faba bean experiments were conducted in southwestern France over several growing seasons (2002-2015) with limited pest, disease and weeds pressure, This dataset provides a rich basis to adapt *STICS* to faba bean and analyse the capacity of the model to unravel the role of abiotic factors in driving yield and N_2 fixation variability. Our first objective was to calibrate and assess the performance of *STICS* to simulate N acquisition by soil mineral uptake and biological N_2 fixation, crop development and shoot biomass production, grain yield formation, N content in grain and straw, and soil water and mineral N contents along the whole profile during crop growth and after harvest. By doing so, we explored the hypothesis that the generic model -(*i.e.* with the same formalism for all crops) can take into account the specificities of faba bean (N_2 fixation) and can be robustly calibrated for this grain legume. The second objective was to analyze the ability of *STICS* to generate a robust prediction for an independent dataset and allow a credible agronomic diagnosis of yield and N_2 fixation variability due to abiotic stresses. For this objective, our hypothesis was thatthe spatio-temporal adequacy of soil/crop relationships (e.g. N nutrition based on both mineral-N uptake and N2 fixation) and the realism of the implemented process equations allow for an accurate prediction of abiotic stresses.

2. Materials and Methods

2.1. *STICS,* a soil-crop model

2.1.1. Overview of the model

The soil–crop model (as well as cropping system model) *STICS* (Brisson et al., 2008, 2002, 1998) was chosen for its agro-environmental purpose, crop genericity (allowing the simulation of crop successions with the same model) and robustness. *STICS* simulates carbon, water and nitrogen dynamics in the soil–crop system on a daily time step over the crop cycle. Unlike crop models that combine crop modules with different structures, *e.g. DSSAT* (Decision Support System for Agrotechnology Transfer, Jones et al., 2003) or *APSIM* (Agricultural Production Systems sIMulator, Keating et al., 2003), *STICS* uses a common and generic structure for different crop species. Species-specific sets of parameters define the differences between species. *STICS* has been adapted and tested for different type of crops (*e.g.* winter wheat, maize, barley, sunflower, rapeseed, grassland, tomato, grapevines) (Coucheney et al., 2015).

Inputs to the model include daily weather information (minimum and maximum temperature, rainfall, wind and global radiation), soil characteristics (per-layer initial soil water and mineral N content, field capacity and wilting point) and crop/soil management (date and depth of planting, planting density, soil tillage, residues management, organic and mineral fertilisation, irrigation).

Crops are defined by species parameters, ecophysiological options (*e.g*. effect of photoperiod and/or cold requirements on crop phenology, potential radiation use efficiency) and cultivar specific parameters (*e.g.* flowering precocity, maximum number of grains per m^2). Crop temperature (calculated from weather variables) and photoperiod drive crop phenology. The model dynamically simulates (i) development of the root system that takes up N and water according to root density over the whole soil profile and (ii) the establishment of the canopy that transpires water and intercepts light to produce the crop biomass.

Two processes account for yield formation in the model: (i) setting of grain number per square meter and (ii) accumulation of biomass in grain. The number of grains before the start of grain filling is a function of: (i) the number of days before the beginning of grain filling during which grain number is determined (crop parameter), (ii) the mean canopy growth rate during this phase (calculated by the model), (iii) the sensitivity of grain onset to growth conditions (crop parameter) and (iv) the maximum number of grain (crop parameter). Dry matter accumulation in grains is calculated by applying a dynamic harvest index (grain to shoot biomass ratio) to the dry weight of the plant (Amir and Sinclair, 1991). This harvest index increases with time from the beginning of grain filling to physiological maturity, the rate of increase being a crop parameter. A maximum final harvest index (crop parameter) prevent unrealistic remobilization levels. A maximum grain yield corresponding to the simulated number of grains multiplied by the maximum weight of one grain (crop parameter) is computed to avoid unrealistic yield level.

The model also accounts for soil water and N dynamics. Net N mineralization from crop residues and soil organic matter (affected by clay and $CaCO_3$ content in the topsoil and governed by soil moisture and temperature), nitrification (affected by pH in the topsoil), nitrate leaching and ammonia and nitrous oxide gaseous emissions are daily simulated as well as vertical water drainage when field capacity is exceeded.

STICS also simulates N acquisition by N_2 fixation for legumes. Nodule formation is a function of soil thermal time and sets the potential fixation. Actual N_2 fixation then depends on shoot growth rate (C limitation for N_2 fixation), soil temperature, soil moisture, and a nitrate inhibition effect linked with nitrate-N concentration in the nodulation layer (see section 2.1.2).

The equations governing physical and biological processes occurring in the soil/crop system are based on a unique set of general parameters. Model parameters and equations describing

yield formation are of particular interest in this study and are described in details in Table S2. An exhaustive description of inputs, equations and default parameter values of the *STICS* model is given in Brisson et al. (2008). Bergez et al. (2014) give an overview of the latest plant and soil process-based developments of the *STICS* model, and Coucheney et al. (2015) detailed the *STICS* version 8.5 used in this study.

2.1.2. Stress factors

Physical and biological processes are successively addressed in two types of equations: 1) the calculation of the potential flux or rate of the process; 2) the effect of the environmental limiting factors, including the stress factors of the crop (light, C, N and water). Four stress factors can indirectly affect grain yield through plant growth. The first is a water stress factor that affects radiation use efficiency and plant transpiration, and is computed as the ratio of actual evapotranspiration over potential evapotranspiration. Potential transpiration is function of Leaf Area Index (LAI) and daily potential Penman evapotranspiration, as calculated by the model. Actual transpiration is calculated as the minimum between water soil supply and maximal crop demand. The second stress factor is a Nitrogen stress that affects 1) LAI increase, 2) radiation use efficiency and 3) possibly senescence. The N stress index is computed as the ratio of actual Nitrogen concentration over Critical crop N concentration. Critical crop N concentration is the minimum N concentration that allow to maximise biomass production (Lemaire and Gastal, 1997). Actual N uptake is calculated as the minimum between soil supply and maximal crop demand. The third stress is a heat reduction factor on radiation use efficiency that increases when daily average crop temperature exceeds optimal crop temperature and is maximal when daily average crop temperature exceeds maximal crop temperature. The fourth is a heat stress factor that stops grain yield when daily average crop temperature exceeds maximal temperature for grain filling.

For legumes, *STICS* also calculates water, heat, anoxia and nitrogen stress factors for N_2 fixation. The water deficit factor for N_2 fixation is the proportion of soil layers in the nodulation area (crop parameter "*profnod*", set to 30 cm in our study) for which moisture is above wilting point. The heat stress factor for N_2 fixation increases and is maximal when soil temperature in nodulation zone exceeds optimal and maximal temperature thresholds. Nitrogen stress for N_2 fixation increases and is maximal when the mean amount of mineral nitrogen in the rooting zone (*i.e.* the upper soil layers where the bacterial symbiosis is the most active) exceeds an optimal or maximal N concentration threshold. Eventually, anoxia stress factor for N_2 fixation increases with the proportion of soil layers in anaerobic conditions.

Stress factors are computed daily and vary between 0 (complete stress) and 1 (no stress). Model parameters and equations used to compute water stress factor and water deficit factor for N_2 fixation are of particular interest in this study and are described in details in Table S2. The exhaustive description of the equations and parameters governing the stresses definition can be found in Brisson et al. (2008).

2.2. Experimental data

2.2.1. Sites and experimental design

The experimental data was collected in south of France at the experimental sites of INRA in Auzeville (43°31'N 1°28'E), and of CREAB-MP in Auch (43°38'N 0°36'E) during seven growing seasons in each site. In both sites, the climate is oceanic temperate under mediterranean influence and characterized by summer droughts and cool wet winters. Cumulative global radiation, growing degree-days and rainfall during crop growth (November-July), averaged across growing seasons, were similar in Auch and Auzeville (Table 1). Experimental plots were in the valley on deep (*i.e.* average maximum rooting depth

213 of 135 cm) clay-loamy soils in Auzeville and on the hillside on shallow (*i.e.* average
214 maximum rooting depth of 70 cm) clay loamy soils in Auch. As a result, average maximum
215 available water to maximum rooting depth (*i.e.* soil water content at field capacity minus soil
216 water content at wilting point) was higher in Auzeville (167 mm) than in Auch (64 mm)
217 (Table 1).

218 Cropping systems strongly differed between experimental sites. In Auzeville, the data
219 originated from two distinct types of experiments. The first type was annual experiments with
220 replicated plots (1.62 m wide x 13m long) of sole faba bean (see Bedoussac and Justes (2010)
221 and Kammoun (2014) for a detailed description of experimental design). The second type was
222 a long-term cropping system experiment established in 2003 on 200 x 30 m plots with
223 different three-years rotations varying in the frequency of grain legumes and the use or not of
224 cover crops (Plaza-Bonilla et al., 2017). Appropriate herbicide and pesticides were applied to
225 control weeds, pests and diseases and no N fertilizer was applied on legumes.In Auch, the
226 data originated from an organic long-term soil fertility monitoring experiment (2002-2013)
227 with 50 x 50 m plots with Faba bean – Oat or wheat – Sunflower rotations (Colomb et al.,
228 2013).Auch was managed without mineral fertiliser, herbicides and pesticides. As a result,
229 only the plots where the monitoring revealed negligible pests, disease and weed pressure were
230 considered. In both sites, the land was plowed prior to sowing and only in 2007 in Auzeville
231 small amounts of irrigation water (20-50mm) was applied after sowing (Table 2) to ensure
232 satisfactory crop establishment.

233 The considered faba bean cultivars were Castel and Irena (Table 2). These winter-type
234 cultivars sown between November and January have similar phenology and yield potential
235 (Flores et al., 2012). Site, year, and management factors (cultivar, crop density, incorporation
236 of a cover crop before planting and sowing date) defined 35 Site-Year-Management units
237 (Table 2). Site-year-management units covering a broad range of soil types, growing seasons

238 and management situations (He et al., 2017) were chosen for the calibration dataset (Table 2).
239 The remaining units, differing in growing season and/or management (compared with
240 calibration dataset) formed the evaluation dataset (Table 2).

241 **2.2.2. Measurements**

242 Faba bean development stages were recorded in the annual experiments in Auzeville
243 following BBCH scale (Meier, 2001), namely (i) BBCH 09: 50% of shoot have emerged
244 through soil surface (ii) BBCH 70: first pods have reached final length (corresponding to
245 "drp" stage in *STICS*, *i.e.* the beginning of grain filling). Additionally, interpolation of
246 discontinuous LAI observations allowed for determining the date of the end of juvenile phase
247 (*amf* stage in STICS, corresponding to maximum growth rate of LAI). The interpolation was
248 carried out with the tool integrated in *STICS* that uses an functional equation to differentiate
249 LAI growth (logistic equation) and senescence (exponential equation), the difference between
250 the two functions giving the green LAI (see Casa et al., 2012, for detailed equations and
251 procedure).

252 In each experimental field, soil texture and pH were measured over the whole soil profile (0-
253 120 cm). Soil mineral N and water content were measured by layers of 30 cm three times per
254 year: (1) end of autumn prior to sowing, (2) mid-winter and (3) at harvest. Crop variables
255 such as LAI, above-ground biomass, fixed N_2 and total accumulated N, grain yield and grain
256 N content were measured from 1 to 5 times depending on site, year and experiment (Table 2):
257 (1) in mid-March *i.e.* wheat '1cm ear' stage, (2) in mid-April, *i.e.* legume flowering, (3) in
258 mid-may *i.e.* wheat flowering, (4) in early June *i.e.* wheat ripening, and (5) in early July, *i.e.*
259 legume maturity. At each measurement, six central rows 0.5 m long (annual experiments in
260 Auzeville), six m^2 (long term cropping system experiment in Auzeville) and nine subplots of
261 two rows 1 m long (in Auch) were harvested by cutting plants at the soil surface. In the annual

experiments in Auzeville, a LI-3100 planimeter (LI-COR, Lincoln, NE) was used to determine green leaf area. In all experiments, plant biomass samples were dried at 80°C for 48 h and weighted. At maturity, plants were threshed to determine grain yield and harvest index. Above-ground plant and grain N concentration were determined on finely ground plant material with the Dumas combustion method using a Leco-2000 analyzer (LECO, St. Joseph, MI, US). In Auzeville, N_2 fixation ratio, *i.e.* the proportion of plant N derived from atmosphere (%Ndfa) was determined using the ^{15}N natural abundance method (Unkovich, 2008) with unfertilized wheat and non-legume weeds as reference plants in the annual and long-term experiments respectively. %Ndfa was calculated as follows:

$$\%\text{Ndfa} = 100 \times \frac{\delta 15N_{ref} - \delta 15N_{fababean}}{\delta 15N_{ref} - \beta} \quad (1)$$

where $\delta^{15}N$ is the deviation from the international standard of atmospheric N_2 (0.3663% ^{15}N) for faba bean ($\delta^{15}N_{faba\ bean}$) and for the reference crop ($\delta^{15}N_{ref}$), and β is the $\delta^{15}N$ of shoots of faba bean fully dependent upon N_2 fixation, assumed equal to −0.63 ‰ (Unkovich, 2008). The amount of N_2 fixed was calculated as the product of %Ndfa and total above-ground plant N.

Moreover, dynamics of maximum rooting depth of faba bean was monitored in 2013 during the annual experiment in Auzeville (Table 2) using a rotary scanner-based minirhizotron system (CI-600, CID Bio-science, Camas, WA, USA) six times during crop growth (16 and 28 March, 12 April, 6 May, 3 June, 17 July).

2.3. Calibration procedure

The calibration consisted in choosing the formalisms and corresponding parameters involved in the simulation of crop phenology, leaf area and root system expansion, biomass accumulation, biological nitrogen fixation, nitrogen uptake and grain yield elaboration.

285 The parameterization procedure included three steps (Figure 1). The first step was a literature
286 review to select the options offered by the model to simulate the different crop processes and
287 determine existing parameter values s. The second step corresponded to the determination of
288 parameters from experimental data by direct measurement or observation (phenology). The
289 last step consisted in a mathematical optimisation based on the approach developed by
290 Guillaume et al. (2011), including nine stages representing the different key processes in the
291 simulation of the final outputs of the model (Table 3). For each stage, sensitivity analysis
292 (Ruget et al., 2002) and expert knowledge were used to select the parameters having the
293 strongest impact on model outputs. In total, 29 crop parameters were mathematically
294 optimised (Table 3). Stage-specific target variables were selected: (i) dates of key
295 development stages (emergence, end of juvenile phase, beginning of grain filling and
296 physiological maturity), (ii) dynamic variables (Leaf Area Index, above-ground biomass,
297 fixed N and total plant N, overall soil moisture content and overall soil N content) and (iii)
298 variables at crop maturity (yield components, grain yield and grain N content) (Table 3). The
299 calibration stages were carried out by using the software package *OptimiSTICS* (Wallach et
300 al., 2011) and the methodology detailed by Buis et al. (2011). Model error was computed as
301 the difference between measured and simulated values for a given target variable at a given
302 date. The goodness of fit C*v* was obtained following the formula:

303 $$C_v = \sum_s \frac{1}{n_s} \sum_i \left[O_{s,i} - P_{s,i}(\theta) \right]^2 \qquad (2)$$

304

305

306 Where *v* is the target variable, *s* is the site-year-management unit and n_s is the number of
307 measurements in *s*, $O_{s,i}$ is the measured value in site-year-management *s* on the ith date and
308 $P_{s,i}(\theta)$ is the corresponding simulated value with the parameter set θ.

This average squared error for a given target variable was minimised using a simplex algorithm. For each optimised parameter, , lower and upper limits corresponding to reasonable physiological values were fixed based on literature and expert knowledge (Table 3). The optimised parameter values at a given stage were the default values of the next steps. The initial plant parameters before optimisation were taken from the spring pea plant file (Corre-Hellou et al., 2009). Given the similarities in crop functioning and yield potential observed in our experiments between the two studied faba bean cultivars (Irena and Castel), we did not calibrate specific cultivar parameters.

Soil analysis informed the input parameters required for soil in *STICS*. Moisture at field capacity and wilting point were first obtained using pedo-transfer functions (Saxton and Rawls, 2006) and also based on laboratory measurements on sieved soil for field capacity, and then adjusted by trial and error to minimize the error between simulated and observed soil water content in mid-winter. The recorded crop managements (Table 2) were used to create management files used for each simulation. Initial soil mineral nitrogen (nitrate ammonium) and water content were measured for each experiment and set between 13 and 120 kg N ha^{-1} and 162 and 342 mm respectively, depending on the different Site-year-management units (Table 2).

2.4. Model evaluation

Model performance (with optimised parameter set) was evaluated graphically and quantified by calculating Mean Bias Error (MBE) and its relative value (rMBE), Model Efficiency (EF), Root Mean Square Error (RMSE) and its relative value (rRMSE):

$$MBE = \frac{1}{n}\sum_{i=1}^{n}(P_i - O_i) \quad (3)$$

$$rMBE = \frac{MBE}{\bar{O}} \times 100 \quad (4)$$

$$EF = 1 - \frac{\sum_{i=1}^{n}(O_i - P_i)^2}{\sum_{i=1}^{n}(O_i - \bar{O})^2} \quad (5)$$

$$RMSE = \sqrt{\frac{1}{n}\sum_{i=1}^{n}(O_i - P_i)^2} \quad (6)$$

$$rRMSE = \frac{RMSE}{\bar{O}} \times 100 \quad (7)$$

where O_i and P_i are the observed and simulated values for the i^{th} measurement, n is the number of observations and $\bar{O}$ is the mean of the observed values.

MBE and rMBE indicate whether the model under/overestimate a given variable, and gives the absolute and relative magnitude and direction of the bias. EF is based on the comparison of the simulation model with a constant model *(i.e*. the average of measured data) and ranges between -∝ and one. Negative EF values indicate that the constant model performs better than or as well as the simulation model. A value of one indicate a perfect model. EF is a good indicator to compare model simulations with two different sets of parameters (*e.g.* before/after calibration) against the same dataset. It is however of little value to compare two simulations with the same set of parameters against two different datasets, because it depends on the variance of the observed dataset. RMSE and rRMSE are the model absolute and relative prediction error. The combined analysis of these four indicators give a robust assessment of model accuracy. Similarly to Beaudoin et al. (2008) and Constantin et al. (2015), model predictions were judged satisfactory when EF value were greater than 0.5 and rMBE lower than 10%. A summary of the calibration and evaluation procedure can be found in Figure 1.

2.5. Stress factors and variability in grain yield and total N_2 fixed

Stress factors calculated by *STICS* (see section 2.1.2 and Table S2) were averaged over periods ranging from -60 to + 60 days before/after the beginning of grain filling. For each

period, the Pearson correlation coefficient (R^2) between observed grain yield (total fixed N_2 respectively) and stress factor affecting grain yield (N_2 fixation respectively) over the period was computed. The period corresponding to the maximum R^2 was determined. For this analysis, calibration and evaluation datasets were pooled.

3. Results

3.1. Parameter values obtained from literature, experimental data and optimisation

Eight parameters values were obtained from literature (Table 4). Faba bean shows a long day response to photoperiod (Ellis et al., 1988) and needs vernalisation (Patrick and Stoddard, 2010) so we activated these physiological options in the faba bean plant file. Faba bean base temperature for crop development (*tdmin*) was set to 0°C (Tribouillois et al., 2016). Because there was no available data in the literature, base and optimal temperature for photosynthesis (*temin* and *teopt*) were approximated from those for emergence rate (Tribouillois et al., 2016) (Table 4), based on the assumption that cardinal temperatures for developmental processes are close for a given species (*e.g.* Parent and Tardieu, 2012). Cardinal temperatures for nodulation (*tempnod1, tempnod2, tempnod3, tempnod4*) were obtained from Boote et al. (2002) (Table 4).

Four parameters values were obtained using direct in-field measurement (Table 4). Maximum and minimum number of grain per square meter (*nbgrmax* and *nbgrmin*), maximum grain weight (*pgrainmaxi*) and maximum harvest index (*irmax*) were set to the maximum or minimum measured values in the experiments in Auzeville and Auch with an added or subtracted 10% respectively to reach assumed potential values (Table 4 and Figure 2).

The other 30 parameters values were set according to the result of the sequential optimisation with *OptimiSTICS* using measured variables (Table 4).

3.2. Agreement between simulated and observed values

3.2.1. Crop development and LAI

Calibration led to satisfactory prediction of the dates of emergence, end of juvenile phase, beginning of grain filling and physiological maturity. Relative bias was low (0 – 10%) with fair EF values (Figure 3), indicating the relevance of calculating crop development based on vernalisation and photoperiodic and thermal time-course formalisms. Simulated LAI values for the calibration dataset were close to observed values with a low relative bias of 1% and a satisfactory EF of 0.69. Prediction error was however great due to a bias of a few days in the senescence dynamic that had large consequences on the daily agreement between observed and simulated LAI values (rRMSE=56%) (Figure 4a).

3.2.2. Above ground biomass, N_2 fixation and N acquisition

Predicted biomass agreed with observation throughout the growth seasons in both calibration and validation datasets (EF>0.77 and -7% < bias < 0%). Prediction error was high due to senescence defoliation between grain physiological maturity and harvest that was difficult to precisely simulate (rRMSE of 41 and 31% for calibration and evaluation respectively). There was a large variation in faba bean biomass at harvest (1.5 - 11.6 t ha^{-1} and 2.8 - 7.2 t ha^{-1} for calibration and evaluation datasets respectively) depending on site, year and management (Figure 4c, d) and the model was able to reproduce this behaviour.

The calibration of parameters related to N_2 fixation (Table 3 and Table 4) allowed to reach a good agreement of simulated versus observed values throughout crop growth (Figure 4e,f) (EF = 0.77 with negligible bias). EF remained high and bias remained low in the evaluation indicating that the model was able to reproduce the wide range of final N_2 fixed at harvest (62-166 kg N ha^{-1}, Figure 4f). N acquired (N content in crop aerial parts) was adequately

simulated with low bias both in calibration and evaluation (-7 and 2% respectively) and EF values above 0.5 (Figure 4g, h).

3.2.3. Grain yield and grain N content

Observed grain yield greatly varied depending on site-year-management (0.42 – 4.7 t ha-^{1}, Figure 5a). The model performed well in simulating grain yield (EF=0.66 with low relative bias) for calibration dataset. Model performance remained satisfactory during evaluation, with an EF value of 0.65 and a relative bias of -1% (Figure 5b).

Simulated grain N content was slightly underestimated (relative bias of -10%) in the calibration dataset with a satisfactory EF value of 0.60 (Figure 5c). In the evaluation, grain N content was predicted with a low relative bias (3%). The EF was low (0.27) but the range of observed values for evaluation (65-162 kg N ha^{-1}) was narrower than for calibration (21-200 kg N ha^{-1}).

3.2.4. Soil water and soil mineral N contents

Soil water content over the entire profile was correctly simulated by the model, both during calibration and evaluation (EF>0.70 with small relative bias) (Figure 5e, f). Soil N content was less adequately predicted, with small (0.22) and negative (-1.42) EF values, in calibration and evaluation respectively (Figure 5g, h). Bias was low in the evaluation (-10%), indicating that though the model was not able to reproduce precisely the differences between site, year and management, it predicted soil mineral N content within the range of the rather low observed values.

3.3. Impact of temporal dynamics of stress factors

With regard to grain yield, the water stress factor (*i.e.* water supply/demand ratio, see section 2.1.2 and Table S2) had the strongest explanatory power. Indeed, when averaged over a

425 period of 6 days before the beginning of grain filling (i.e. the end of grain onset), it explained
426 78% of the observed grain yield variability in the overall dataset (Figure 6a). The model fairly
427 reproduced the temporal dynamic of above ground biomass (Figure 7d, e, f). Water stress
428 during the end of grain onset (Figure 7a, b, c) affected the growth rate of above ground
429 biomass (Figure 7d, e, f), which in turn influenced the final number of grains (Figure 7g, h, i).
430 In the end, the model was able to simulate contrasting water stresses that occurred in different
431 soil types (valley/hillside) for a range of climatic conditions and their final impact on the
432 number of grain and grain yield (Figure 7). Heat stress effect on radiation use efficiency,
433 conversely, had a limited explanatory power in our conditions. Indeed, when averaged over a
434 period of 26 days after the beginning of grain filling (the period with the best correlation),
435 heat stress explained only 25% of the observed grain yield variability. The model diagnosed
436 no heat stress on grain filling in the majority of the site-year-management units. There were
437 only five days in 2002 in Auch during which crop temperature exceeded the maximal
438 temperature above which grain filling stops (Figure S1).

439 With regard to N_2 fixation, the water deficit factor had also the strongest explanatory power.
440 Thus, when averaged over a period of 20 days after the beginning of grain filling, it explained
441 82% of the observed variability in total fixed N_2 at harvest (Figure 6b). Despite a limited
442 number of within-season measurements in some situations (Figure 8d), the model reproduced
443 reasonably well the temporal dynamic of N_2 fixation (Figure 8c, d). In the end, the model was
444 able to reproduce the wide range of total fixed N_2 at harvest (62-172 kg ha^{-1}, see Figure 6).
445 The model diagnosed no stress due to anoxia in any of the cropping situations of this study.
446 Though the model diagnosed limited heat and nitrogen stresses in some situations (value of
447 0.67 and 0.58 respectively) the correlation with the amount of N_2 fixed was not significant for
448 any of the periods considered.

449 **4. Discussion**

4.1. A method to adapt a generic crop model to a new crop

While the process of calibrating a new cultivar is well described (*e.g.* (Jégo et al., 2010), less emphasis has been put on the description of the adaptation of a generic soil-crop model to a new crop. Previous studies mainly described a partial calibration based on a limited set of target variables, *e.g.* LAI or AGB and Soil water (Confalonieri and Bechini, 2004; Ko et al., 2009), and did not address the broad range of processes available in the model (*e.g.* root system expansion, Nitrogen uptake, yield formation). Our study shows that the generic *STICS* soil-crop model can be successfully adapted to a new crop, and in particular a grain legume having the specificity of N_2 fixation. The adaptation was based on two steps, namely: (i) a parameter estimation based on measurement and literature and (ii) a sound and careful sequential optimisation of crop parameters that were not measured nor estimated using existing literature. Therefore, our work contributes to establish a generic method to calibrate a new annual crop for soil-crop models that (i) have a common structure for different crop species, (ii) are functional deterministic models considering water, C and N cycles, on a daily time step (Di Paola et al., 2016) and (iii) have an available parameter optimisation tool.

Estimating a parameter from direct measurements and literature has the advantage of not being based on the assumption that model formalism and all other parameters are reliable, as it is the case with mathematical optimisation (Grant, 2001). It should be therefore prioritised and in our approach we had 9 parameters estimated in this way (Table 4). However, this procedure is not always possible for many reasons. Firstly, field measurements of parameters is expensive and time consuming (Anothai et al., 2008). Secondly, the dataset used for model calibration may not be originally intended to cover model calibration issues (as it was the case in our study), so that most of crop model parameters are not directly measured (*e.g.* radiation use efficiency). Thirdly, the need for similar environmental conditions, varieties and exact correspondence of the measured variable to the process represented by the model limit the

475 number of parameters that can be derived from a literature review. For example, the radiation
476 use efficiency parameters in *STICS* (*efcroijuv*, *efcroiveg* and *efcroirepro,* see Table 3)
477 correspond to potential conditions with no stress, and the presence or absence of stress is not
478 necessarily mentioned in the literature. Finally, there is a risk of error accumulation when
479 extensively relying on approximate or conflicting literature values (Wallach et al., 2011). For
480 all these reasons, recourse to optimisation is advisable. The strength of our approach lies in
481 the rational stepwise optimisation procedure chosen. Rather than an empirical trial and error
482 procedure (Flénet et al., 2004; Hartkamp et al., 2002), we chose a sequential optimisation
483 procedure that is fully documented and is easily replicable for other crops and cultivars with
484 the *STICS* model. =Breaking down the optimisation into several stages and using it at the
485 module-scale rather than the scale of the entire model allow to avoid unrealistic simulations
486 where errors in parameter values would offset each other (Bechini et al., 2006; Grant, 2001).
487 Taking into account within-season dynamic measurements to successively calibrate the
488 different model components allows to estimate few parameters simultaneously and therefore
489 to reduce numerical problems (Guillaume et al., 2011; Wallach et al., 2011). The lower and
490 upper boundaries fixed for each parameter during the optimisation ensures that the obtained
491 values correspond to reasonable physiological values thus limiting compensations due to
492 model structure weaknesses. The different optimisation stages and their order following crop
493 development (*i.e.* phenology, LAI, biomass production and then partitioning) ensure that the
494 parameterisation is relevant according to plant functioning. The order chosen is consistent
495 with previously published calibrations using *STICS* (Corre-Hellou et al., 2009; Flénet et al.,
496 2004) and *DSSAT* (Hartkamp et al., 2002). Finally this method led to a satisfactory match of
497 observed and simulated values, with ranges for statistical indicators (EF, rMBE and rRMSE)
498 consistent with those obtained for the adaption of *STICS* to wheat and maize (Brisson et al.,
499 2002), linseed (Flénet et al., 2004) and spring pea (Corre-Hellou et al., 2009). This approach

500 can be valuable to calibrate new annual crops and other grain legumes (*e.g.* winter pea, lentil
501 and chick pea) for the *STICS* model, and probably other generic soil-crop models that have a
502 common structure for all species, *e.g. CROPSYST* model (Stöckle et al., 2003).

503 **4.2. A robust and credible agronomic diagnosis**

504 Agronomic diagnosis is crucial for the identification of constraints affecting crop growth and
505 to help the identification of sound agronomic management. The diagnosis needs to be robust,
506 *i.e.* reliable under different sets of experimental conditions (Sinclair and Seligman, 2000), and
507 credible, *i.e.* offering trustworthy causal explanations (Cash et al., 2002). Robustness can be
508 ensured by an explicit reference to physical processes in the construction of mathematical
509 relationships so that the model accurately captures the underlying processes driving the
510 system (Bellocchi et al., 2010). Lack of robustness can lead to a model being "right for the
511 wrong reasons" (Bellocchi et al., 2010). In this section, we want to highlight that we averted
512 these pitfalls, ensuring that our diagnosis was robust and credible.
513 Our study adds to the body of literature showing that in a temperate climate with rain fed
514 conditions and appropriate control of pest pressure, drought is the prevailing stress and the
515 main driver of yield variability (Karrou and Oweis, 2012; Mafakheri et al., 2010). The
516 explanations we found to explain yield variability (water stress during grain onset) and N_2
517 fixation variability (water deficit factor during grain filling) are supported by principles of
518 crop physiology derived from experiments and knowledge on response of legume grain yield
519 and N_2 fixation to water stress. With regard to grain yield, water deficit during grain onset
520 reduces grain legume biomass accumulation (decrease of photosynthesis and reduction of leaf
521 area) and assimilate availability that in turn reduce final seed number (Guilioni et al., 2003;
522 Jiang and Egli, 1995; Lake and Sadras, 2016). With regard to N_2 fixation, water stress directly
523 reduce faba bean nodules activity (Sprent, 1972) and sensitivity of N_2 fixation to drought is
524 often maximum during grain filling (Chalk et al., 2010; Mastrodomenico et al., 2013). These

two stress responses are implemented in *STICS*. Firstly, final seed number depends on plant growth rate during the grain onset period (see section 2.1.1 and Table S2). . Thus, the magnitude of water stress during grain set and its impact on plant growth rate determines the extent to which the plant can reach the maximum grain number (*nbgrmax*, see Table and Figure 2). Secondly, in the model, water deficit reduces the potential N_2 fixation, *i.e.* nodulation and nitrogen fixation are partially or totally inhibited according to nitrate concentration in the topsoil and when soil moisture in the topsoil drops below permanent wilting point (see section 2.1.2 and Table S2). This careful check of the behaviour of different model functional modules (Figure 7, Figure 8) strongly suggests that the *STICS* model accurately captured the underlying processes driving grain yield formation, N_2 fixation and water stress. We can therefore be confident in the diagnosis drawn from our site-year-management units with regard to water stress. Thus, the generic *STICS* processes describing yield formation and water stress, when calibrated for faba bean with the proper options activated, have proven useful in explaining variability in yield for this particular legume crop, without the need to build new processes into the generic model.

The good fit obtained with the evaluation dataset indicates that the current set of parameters could be reliably used in other situations different from the ones in the calibration. This however needs to be confirmed with other studies, *e.g.* for situations where soil mineral N levels would be higher than in our study (on average 47 kg ha^{-1} at sowing over the whole profile), which could affect N_2 fixation. We verified by virtual experiment - corresponding to a local sensitivity analysis - that *STICS* was able to simulate a strong reduction in N_2 fixation when soil nitrate content was higher in the upper layers.

Eventually, by considering both a water deficit factor for N_2 fixation and a water supply/demand ratio (acting on crop biomass), the model allowed unravelling interesting situations where similar faba bean biomass masked differences in the amounts of fixed N_2.For

example, crop biomass and water/supply demand ratio were similarly low in Auzeville in 2011 (3 t ha^{-1}) and 2015 (4.1 t ha^{-1}) due to similar water stress on biomass (water supply-demand ratio = 0.3). However, the amount of N_2 fixed was doubled (88 kg ha^{-1}) in 2015 compared with 2011 (46 kg ha^{-1}). The model indicated a stronger water deficit for N_2 fixation in 2011 (water deficit factor = 0.12) compared with 2015 (water deficit factor = 0.32). This understanding of nonlinearities is crucial for the assessment of innovative cropping system.

Pests and diseases can also reduce faba bean grain yield. Coupling *STICS* with an epidemiological model (Donatelli et al., 2017) would be relevant to refine the diagnosis in situations where damages on leaves (*e.g.* rust, *Uromyces viciae-fabae,* or chocolate spot, *Botrytis fabae*) and nodules (*e.g.* sitonia beetles, *Sitonia lineatus*) can occur.

4.3. New opportunities to design and assess resilient cropping systems

Though the effects of climate change on cereals in Europe have deserved a great attention (*e.g.* Bregaglio et al., 2017; Dettori et al., 2017), studies on effects of climate change on legume productivity remain scarce. Climate change projections for the temperate and mediterranean regions of Europe point to a decrease in precipitations during spring and summer (Gao and Giorgi, 2008; Giannakopoulos et al., 2009). Water stress will therefore become even more acute with future climate. Our model calibration offers a good opportunity to assess the impact of increased drought-induced stress on faba bean productivity and therefore the potential contribution of legume to sustainable cropping systems in the future.

Dynamic models have often been criticised for putting too much emphasis on single crop assessment on a year-to-year basis (Reckling et al., 2016). Taking into account pre-crop and rotational effects (*e.g.* nutrient carry-over and alteration of soil water content) will be crucial to accurately assess the contribution of faba bean and grain legumes in building more diversified and resilient cropping systems. Our robust crop calibration and *STICS* ability to

575 simulate residues mineralisation (Justes et al., 2009), nitrate leaching and water drainage
576 (Plaza-Bonilla et al., 2015), would allow deriving probabilities to achieve a certain level of
577 yield and N provision to the subsequent crop when inserting legumes in cropping systems.

578 *STICS* can also simulate intercropping (Brisson et al., 2008). Cereal-legume intercropping
579 (*e.g.* wheat and faba bean) is a promising integration of legumes in cropping systems in
580 particular in low input cropping systems (Bedoussac et al., 2015). Many processes (e.g. soil N
581 and water sharing) are simulated similarly in sole crop and intercrops (Corre-Hellou et al.,
582 2009), our calibration would therefore allow exploring intercropping performance for a
583 diversity of soils and rainfall patterns. Nevertheless, some formalisms specific to intercrops
584 (*e.g.* the competition for light) and the corresponding parameters may deserve potential re-
585 calibration before the set of parameters proposed here for sole crops can be used.
586

587 **Conclusion**

588 Based on literature and cropping experiments in two contrasting sites of southwestern France,
589 we successfully adapted the *STICS* soil-crop model to faba bean.We developed and validated
590 a method smartly combining the mobilization of literature references, direct field
591 measurements and a transparent and sequential optimisation procedure to derive crop
592 parameters . The obtained set of parameters allowed a satisfactory prediction of plant growth,
593 N_2 fixation, mineral N uptake, grain yield and grain N content. Careful assessment of dynamic
594 variables (plant growth, grain number, N_2 fixation) and the associated stress factors allowed to
595 carry-out a credible and robust diagnosis of grain yield and N_2 fixation variability in the sites
596 of this study. The proposed set of parameter could then be used for (i)(i) yield gap analysis in
597 organic fields affected by biotic as well as abiotic stress,, (ii) exploration studies on the effect
598 of climate change and more frequent droughts on faba bean, and (iii) the effect of its insertion
599 in crop rotations (as sole crop or intercrop) on N provision to the subsequent crop. Calibration

of other grain legumes like chickpea and lentils using the proposed methodology will broaden the capacity of the *STICS* model to simulate innovative cropping systems including grain legumes.

Acknowledgments:

This research was supported by the European Commission (REA) through the LEGATO project (FP7-613551) and the French National Research Agency (ANR) through the LEGITIMES French project (ANR-13-AGRO-0004), the 7th PIREN-Seine program and the Climate-CAFE European project (selected by the European FACCE-JPI ERA-NET Plus program).

We thank the Centre Régional de Recherche et d'Expérimentation en Agriculture Biologique de Midi-Pyrénées (CREAB-MP) in Auch, France, for making available their faba bean dataset. We are grateful to Loïc Prieur, Didier Rafaillac, Michel Labarrère and several trainees who assisted in data collection and Didier Chesneau and Eric Lecloux who performed the extraction and the analysis of soil mineral N. We thank Patrice Lecharpentier for his help with the *Optimistics* software.

References

Affholder, F., Scopel, E., Neto, J., Capillon, A., 2003. Diagnosis of the productivity gap using a crop model. Methodology and case study of small-scale maize production in central Brazil. Agronomie 23, 305–325.

Amir, J., Sinclair, T.R., 1991. A model of the temperature and solar-radiation effects on spring wheat growth and yield. Field Crops Res. 28, 47–58. https://doi.org/10.1016/0378-4290(91)90073-5

Anothai, J., Patanothai, A., Jogloy, S., Pannangpetch, K., Boote, K.J., Hoogenboom, G., 2008. A sequential approach for determining the cultivar coefficients of peanut lines using end-of-season data of crop performance trials. Field Crops Res. 108, 169–178. https://doi.org/10.1016/j.fcr.2008.04.012

Beaudoin, N., Launay, M., Sauboua, E., Ponsardin, G., Mary, B., 2008. Evaluation of the soil crop model STICS over 8 years against the "on farm" database of Bruyères catchment. Eur. J. Agron. 29, 46–57. https://doi.org/10.1016/j.eja.2008.03.001

Bécel, C., Munier-Jolain, N.M., Nicolardot, B., 2015. Assessing nitrate leaching in cropping systems based on integrated weed management using the STICS soil–crop model. Eur. J. Agron. 62, 46–54. https://doi.org/10.1016/j.eja.2014.09.005

Bechini, L., Bocchi, S., Maggiore, T., Confalonieri, R., 2006. Parameterization of a crop growth and development simulation model at sub-model components level. An example for winter wheat (Triticum aestivum L.). Environ. Model. Softw. 21, 1042–1054. https://doi.org/10.1016/j.envsoft.2005.05.006

Bedoussac, L., Journet, E.-P., Hauggaard-Nielsen, H., Naudin, C., Corre-Hellou, G., Jensen, E.S., Prieur, L., Justes, E., 2015. Ecological principles underlying the increase of productivity achieved by cereal-grain legume intercrops in organic farming. A review. Agron. Sustain. Dev. 35, 911–935.

Bedoussac, L., Justes, E., 2010. The efficiency of a durum wheat-winter pea intercrop to improve yield and wheat grain protein concentration depends on N availability during early growth. Plant Soil 330, 19–35. https://doi.org/10.1007/s11104-009-0082-2

Bellocchi, G., Rivington, M., Donatelli, M., Matthews, K., 2010. Validation of biophysical models: issues and methodologies. A review. Agron. Sustain. Dev. 30, 109–130. https://doi.org/10.1051/agro/2009001

Bergez, J.E., Raynal, H., Launay, M., Beaudoin, N., Casellas, E., Caubel, J., Chabrier, P., Coucheney, E., Dury, J., Garcia de Cortazar-Atauri, I., Justes, E., Mary, B., Ripoche, D., Ruget, F., 2014. Evolution of the STICS crop model to tackle new environmental issues: New formalisms and integration in the modelling and simulation platform RECORD. Environ. Model. Softw. 62, 370–384. https://doi.org/10.1016/j.envsoft.2014.07.010

Bishop, J., Potts, S.G., Jones, H.E., 2016. Susceptibility of Faba Bean (Vicia faba L.) to Heat Stress During Floral Development and Anthesis. J. Agron. Crop Sci. 202, 508–517. https://doi.org/10.1111/jac.12172

Boote, K.J., Mínguez, M.I., Sau, F., 2002. Adapting the CROPGRO legume model to simulate growth of faba bean. Agron. J. 94, 743–756.

Bregaglio, S., Hossard, L., Cappelli, G., Resmond, R., Bocchi, S., Barbier, J.-M., Ruget, F., Delmotte, S., 2017. Identifying trends and associated uncertainties in potential rice production under climate change in Mediterranean areas. Agric. For. Meteorol. 237–238, 219–232. https://doi.org/10.1016/j.agrformet.2017.02.015

Brisson, N., Launay, M., Mary, B., Beaudoin, N., 2009. Conceptual Basis, Formalisations and Parameterization of the Stics Crop Model. Editions Quae.

Brisson, N., Mary, B., Ripoche, D., Jeuffroy, M.H., Ruget, F., Nicoullaud, B., Gate, P., Devienne-Barret, F., Antonioletti, R., Durr, C., others, 1998. STICS: a generic model for the simulation of crops and their water and nitrogen balances. I. Theory and parameterization applied to wheat and corn. Agronomie 18, 311–346.

Brisson, N., Ruget, F., Gate, P., Lorgeou, J., Nicoullaud, B., Tayot, X., Plenet, D., Jeuffroy, M.-H., Bouthier, A., Ripoche, D., Mary, B., Justes, E., 2002. STICS: a generic model for simulating crops and their water and nitrogen balances. II. Model validation for wheat and maize. Agronomie 22, 69–92. https://doi.org/10.1051/agro:2001005

Bruelle, G., Affholder, F., Abrell, T., Ripoche, A., Dusserre, J., Naudin, K., Tittonell, P., Rabeharisoa, L., Scopel, E., 2017. Can conservation agriculture improve crop water availability in an erratic tropical climate producing water stress? A simple model applied to upland rice in Madagascar. Agric. Water Manag. 192, 281–293. https://doi.org/10.1016/j.agwat.2017.07.020

Buis, S., Wallach, D., Guillaume, S., Varella, H., Lecharpentier, P., Launay, M., Guerif, M., Bergez, J.-E., Justes, E., 2011. The STICS crop model and associated software for analysis, parameterization, and evaluation, in: Methods of Introducing System Models into Agricultural Research - Advances in Agricultural Systems Modeling 2. L.R. Ahuja Liwang Ma, pp. 395–426.

Casa, R., Varella, H., Buis, S., Guérif, M., De Solan, B., Baret, F., 2012. Forcing a wheat crop model with LAI data to access agronomic variables: Evaluation of the impact of model and LAI uncertainties and comparison with an empirical approach. Eur. J. Agron. 37, 1–10. https://doi.org/10.1016/j.eja.2011.09.004

Cash, D., Clark, W.C., Alcock, F., Dickson, N.M., Eckley, N., Jäger, J., 2002. Salience, Credibility, Legitimacy and Boundaries: Linking Research, Assessment and Decision Making (SSRN Scholarly Paper No. ID 372280). Social Science Research Network, Rochester, NY.

Chalk, P.M., Alves, B.J.R., Boddey, R.M., Urquiaga, S., 2010. Integrated effects of abiotic stresses on inoculant performance, legume growth and symbiotic dependence estimated by 15N dilution. Plant Soil 328, 1–16. https://doi.org/10.1007/s11104-009-0187-7

Colomb, B., Jouany, C., Prieur, L., 2013. Des bilans de phosphore majoritairement négatifs pour les systèmes de grandes cultures biologiques sans élevage en Midi-Pyrénées. Quels impacts sur le phosphore biodisponible des sols et l'état de nutrition des cultures? Innov. Agron. 32, 73–82.

Confalonieri, R., Bechini, L., 2004. A preliminary evaluation of the simulation model CropSyst for alfalfa. Eur. J. Agron. 21, 223–237. https://doi.org/10.1016/j.eja.2003.08.003

Constantin, J., Dürr, C., Tribouillois, H., Justes, E., 2015a. Catch crop emergence success depends on weather and soil seedbed conditions in interaction with sowing date: A simulation study using the SIMPLE emergence model. Field Crops Res. 176, 22–33. https://doi.org/10.1016/j.fcr.2015.02.017

Constantin, J., Le Bas, C., Justes, E., 2015b. Large-scale assessment of optimal emergence and destruction dates for cover crops to reduce nitrate leaching in temperate conditions using the STICS soil–crop model. Eur. J. Agron. 69, 75–87. https://doi.org/10.1016/j.eja.2015.06.002

Corre-Hellou, G., Faure, M., Launay, M., Brisson, N., Crozat, Y., 2009. Adaptation of the STICS intercrop model to simulate crop growth and N accumulation in pea–barley intercrops. Field Crops Res. 113, 72–81. https://doi.org/10.1016/j.fcr.2009.04.007

Coucheney, E., Buis, S., Launay, M., Constantin, J., Mary, B., García de Cortázar-Atauri, I., Ripoche, D., Beaudoin, N., Ruget, F., Andrianarisoa, K.S., Le Bas, C., Justes, E., Léonard, J., 2015. Accuracy, robustness and behavior of the STICS soil–crop model for plant, water and nitrogen outputs: Evaluation over a wide range of agro-environmental conditions in France. Environ. Model. Softw. 64, 177–190. https://doi.org/10.1016/j.envsoft.2014.11.024

Daryanto, S., Wang, L., Jacinthe, P.-A., 2017. Global synthesis of drought effects on cereal, legume, tuber and root crops production: A review. Agric. Water Manag., Special Issue on Improving Agricultural Water Productivity to Ensure Food Security under Changing Environments Overseen by: Brent Clothier 179, 18–33. https://doi.org/10.1016/j.agwat.2016.04.022

716 Dettori, M., Cesaraccio, C., Duce, P., 2017. Simulation of climate change impacts on production and
717 phenology of durum wheat in Mediterranean environments using CERES-Wheat model. Field
718 Crops Res. 206, 43–53. https://doi.org/10.1016/j.fcr.2017.02.013
719 Di Paola, A., Valentini, R., Santini, M., 2016. An overview of available crop growth and yield models
720 for studies and assessments in agriculture. J. Sci. Food Agric. 96, 709–714.
721 https://doi.org/10.1002/jsfa.7359
722 Donatelli, M., Magarey, R.D., Bregaglio, S., Willocquet, L., Whish, J.P.M., Savary, S., 2017. Modelling
723 the impacts of pests and diseases on agricultural systems. Agric. Syst. 155, 213–224.
724 https://doi.org/10.1016/j.agsy.2017.01.019
725 Ellis, R.H., Summerfield, R.J., Roberts, E.H., 1988. Effects of Temperature, Photoperiod and Seed
726 Vernalization on Flowering in Faba Bean Vicia faba. Ann. Bot. 61, 17–27.
727 https://doi.org/10.1093/oxfordjournals.aob.a087524
728 Flénet, F., Villon, P., Ruget, F., 2004. Methodology of adaptation of the STICS model to a new crop:
729 spring linseed (Linum usitatissimum, L.). Agronomie 24, 367–381.
730 https://doi.org/10.1051/agro:2004032
731 Flores, F., Nadal, S., Solis, I., Winkler, J., Sass, O., Stoddard, F.L., Link, W., Raffiot, B., Muel, F.,
732 Rubiales, D., 2012. Faba bean adaptation to autumn sowing under European climates. Agron.
733 Sustain. Dev. 32, 727–734. https://doi.org/10.1007/s13593-012-0082-0
734 Gao, X., Giorgi, F., 2008. Increased aridity in the Mediterranean region under greenhouse gas forcing
735 estimated from high resolution simulations with a regional climate model. Glob. Planet.
736 Change 62, 195–209. https://doi.org/10.1016/j.gloplacha.2008.02.002
737 Giannakopoulos, C., Le Sager, P., Bindi, M., Moriondo, M., Kostopoulou, E., Goodess, C.M., 2009.
738 Climatic changes and associated impacts in the Mediterranean resulting from a 2 °C global
739 warming. Glob. Planet. Change 68, 209–224.
740 https://doi.org/10.1016/j.gloplacha.2009.06.001
741 Grant, F.R., 2001. . Modeling transformations of soil organic carbon and nitrogen at different scales
742 of complexity., in: Ma, L., Hansen, S., Shaffer, M.J. (Eds.), Modeling Carbon and Nitrogen
743 Dynamics for Soil Management. Lewis Publishers.
744 Guilioni, L., Wery, J., Lecoeur, J., 2003. High temperature and water deficit may reduce seed number
745 in field pea purely by decreasing plant growth rate. Funct. Plant Biol.
746 Guillaume, S., Bergez, J.-E., Wallach, D., Justes, E., 2011. Methodological comparison of calibration
747 procedures for durum wheat parameters in the STICS model. Eur. J. Agron. 35, 115–126.
748 https://doi.org/10.1016/j.eja.2011.05.003
749 Hartkamp, A.D., Hoogenboom, G., White, J.W., 2002. Adaptation of the CROPGRO growth model to
750 velvet bean (Mucuna pruriens): I. Model development. Field Crops Res. 78, 9–25.
751 https://doi.org/10.1016/S0378-4290(02)00091-6
752 Hayman, P.T., Whitbread, A.M., Gobbett, D.L., 2010. The impact of El Niño Southern Oscillation on
753 seasonal drought in the southern Australian grainbelt. Crop Pasture Sci. 61, 528–539.
754 https://doi.org/10.1071/CP09221
755 He, D., Wang, E., Wang, J., Robertson, M.J., 2017. Data requirement for effective calibration of
756 process-based crop models. Agric. For. Meteorol. 234–235, 136–148.
757 https://doi.org/10.1016/j.agrformet.2016.12.015
758 Jégo, G., Pattey, E., Bourgeois, G., Morrison, M.J., Drury, C.F., Tremblay, N., Tremblay, G., 2010.
759 Calibration and performance evaluation of soybean and spring wheat cultivars using the
760 STICS crop model in Eastern Canada. Field Crops Res. 117, 183–196.
761 https://doi.org/10.1016/j.fcr.2010.03.008
762 Jensen, E.S., Peoples, M.B., Hauggaard-Nielsen, H., 2010. Faba bean in cropping systems. Field Crops
763 Res., Faba Beans in Sustainable Agriculture 115, 203–216.
764 https://doi.org/10.1016/j.fcr.2009.10.008
765 Jiang, H. (University of K., Egli, D.B., 1995. Soybean seed number and crop growth rate during
766 flowering. Agron. J. USA.

767 Jones, J.., Hoogenboom, G., Porter, C.., Boote, K.., Batchelor, W.., Hunt, L.., Wilkens, P.., Singh, U.,
768 Gijsman, A.., Ritchie, J.., 2003. The DSSAT cropping system model. Eur. J. Agron. 18, 235–265.
769 https://doi.org/10.1016/S1161-0301(02)00107-7
770 Justes, E., Mary, B., Nicolardot, B., 2009. Quantifying and modelling C and N mineralization kinetics of
771 catch crop residues in soil: parameterization of the residue decomposition module of STICS
772 model for mature and non mature residues. Plant Soil 325, 171–185.
773 https://doi.org/10.1007/s11104-009-9966-4
774 Kammoun, B., 2014. Analyse des interactions génotype x environnement x conduite culturale de
775 peuplement bi-spécifique de cultures associées de blé dur et de légumineuses à graines, à
776 des fins de choix variétal et d'optimisation de leurs itinéraires techniques. École Doctorale
777 Sciences Écologiques, Vétérinaires, Agronomiques et Bioingénieries (Toulouse); 154236330.
778 Karrou, M., Oweis, T., 2012. Water and land productivities of wheat and food legumes with deficit
779 supplemental irrigation in a Mediterranean environment. Agric. Water Manag. 107, 94–103.
780 https://doi.org/10.1016/j.agwat.2012.01.014
781 Keating, B.., Carberry, P.., Hammer, G.., Probert, M.., Robertson, M.., Holzworth, D., Huth, N..,
782 Hargreaves, J.N.., Meinke, H., Hochman, Z., McLean, G., Verburg, K., Snow, V., Dimes, J..,
783 Silburn, M., Wang, E., Brown, S., Bristow, K.., Asseng, S., Chapman, S., McCown, R..,
784 Freebairn, D.., Smith, C.., 2003. An overview of APSIM, a model designed for farming systems
785 simulation. Eur. J. Agron. 18, 267–288. https://doi.org/10.1016/S1161-0301(02)00108-9
786 Khan, H.R., Paull, J.G., Siddique, K.H.M., Stoddard, F.L., 2010. Faba bean breeding for drought-
787 affected environments: A physiological and agronomic perspective. Field Crops Res. 115,
788 279–286. https://doi.org/10.1016/j.fcr.2009.09.003
789 Ko, J., Piccinni, G., Guo, W., Steglich, E., 2009. Parameterization of EPIC crop model for simulation of
790 cotton growth in South Texas. J. Agric. Sci. 147, 169–178.
791 https://doi.org/10.1017/S0021859608008356
792 Lake, L., Sadras, V.O., 2016. Screening chickpea for adaptation to water stress: Associations between
793 yield and crop growth rate. Eur. J. Agron. 81, 86–91.
794 https://doi.org/10.1016/j.eja.2016.09.003
795 Lemaire, G., Gastal, F., 1997. N Uptake and Distribution in Plant Canopies, in: Diagnosis of the
796 Nitrogen Status in Crops. Springer, Berlin, Heidelberg, pp. 3–43. https://doi.org/10.1007/978-
797 3-642-60684-7_1
798 Liu, Y., Wu, L., Baddeley, J.A., Watson, C.A., 2011. Models of biological nitrogen fixation of legumes. A
799 review. Agron. Sustain. Dev. 31, 155–172. https://doi.org/10.1051/agro/2010008
800 López-Bellido, R.J., López-Bellido, L., Benítez-Vega, J., Muñoz-Romero, V., López-Bellido, F.J.,
801 Redondo, R., 2011. Chickpea and faba bean nitrogen fixation in a Mediterranean rainfed
802 Vertisol: Effect of the tillage system. Eur. J. Agron. 34, 222–230.
803 https://doi.org/10.1016/j.eja.2011.01.005
804 Mafakheri, A., Siosemardeh, A., Bahramnejad, B., Struik, P.C., Sohrabi, Y., 2010. Effect of drought
805 stress on yield, proline and chlorophyll contents in three chickpea cultivars. Aust. J. Crop Sci.
806 4, 580–585.
807 Mastrodomenico, A.T., Purcell, L.C., Andy King, C., 2013. The response and recovery of nitrogen
808 fixation activity in soybean to water deficit at different reproductive developmental stages.
809 Environ. Exp. Bot. 85, 16–21. https://doi.org/10.1016/j.envexpbot.2012.07.006
810 Meier, U., 2001. Growth stages of mono-and dicotyledonous plants: BBCH Monograph. Fed. Biol. Res.
811 Cent. Agric. For.
812 Meynard, J.-M., Jeuffroy, M.-H., Le Bail, M., Lefèvre, A., Magrini, M.-B., Michon, C., 2017. Designing
813 coupled innovations for the sustainability transition of agrifood systems. Agric. Syst. 157,
814 330–339. https://doi.org/10.1016/j.agsy.2016.08.002
815 Parent, B., Tardieu, F., 2012. Temperature responses of developmental processes have not been
816 affected by breeding in different ecological areas for 17 crop species. New Phytol. 194, 760–
817 774. https://doi.org/10.1111/j.1469-8137.2012.04086.x

Patrick, J.W., Stoddard, F.L., 2010. Physiology of flowering and grain filling in faba bean. Field Crops Res., Faba Beans in Sustainable Agriculture 115, 234–242. https://doi.org/10.1016/j.fcr.2009.06.005

Plaza-Bonilla, D., Nolot, J.-M., Raffaillac, D., Justes, E., 2017. Innovative cropping systems to reduce N inputs and maintain wheat yields by inserting grain legumes and cover crops in southwestern France. Eur. J. Agron., Farming systems analysis and design for sustainable intensification: new methods and assessments 82, Part B, 331–341. https://doi.org/10.1016/j.eja.2016.05.010

Plaza-Bonilla, D., Nolot, J.-M., Raffaillac, D., Justes, E., 2015. Cover crops mitigate nitrate leaching in cropping systems including grain legumes: Field evidence and model simulations. Agric. Ecosyst. Environ. 212, 1–12. https://doi.org/10.1016/j.agee.2015.06.014

Prasad, P.V.V., Bheemanahalli, R., Jagadish, S.V.K., 2017. Field crops and the fear of heat stress—Opportunities, challenges and future directions. Field Crops Res. 200, 114–121. https://doi.org/10.1016/j.fcr.2016.09.024

Reckling, M., Hecker, J.-M., Bergkvist, G., Watson, C.A., Zander, P., Schläfke, N., Stoddard, F.L., Eory, V., Topp, C.F.E., Maire, J., Bachinger, J., 2016. A cropping system assessment framework—Evaluating effects of introducing legumes into crop rotations. Eur. J. Agron. 76, 186–197. https://doi.org/10.1016/j.eja.2015.11.005

Rubiales, D., Fondevilla, S., Chen, W., Gentzbittel, L., Higgins, T.J.V., Castillejo, M.A., Singh, K.B., Rispail, N., 2015. Achievements and Challenges in Legume Breeding for Pest and Disease Resistance. Crit. Rev. Plant Sci. 34, 195–236. https://doi.org/10.1080/07352689.2014.898445

Ruget, F., Brisson, N., Delécolle, R., Faivre, R., 2002. Sensitivity analysis of a crop simulation model, STICS, in order to choose the main parameters to be estimated. Agronomie 22, 133–158. https://doi.org/10.1051/agro:2002009

Saxton, K.E., Rawls, W.J., 2006. Soil water characteristic estimates by texture and organic matter for hydrologic solutions. Soil Sci. Soc. Am. J. 70, 1569–1578. https://doi.org/10.2136/sssaj2005.0117

Sinclair, T.R., Seligman, N., 2000. Criteria for publishing papers on crop modeling. Field Crops Res. 68, 165–172. https://doi.org/10.1016/S0378-4290(00)00105-2

Sprent, J.I., 1972. The Effects of Water Stress on Nitrogen-Fixing Root Nodules. New Phytol. 71, 603–611. https://doi.org/10.1111/j.1469-8137.1972.tb01270.x

Stoate, C., Báldi, A., Beja, P., Boatman, N.D., Herzon, I., van Doorn, A., de Snoo, G.R., Rakosy, L., Ramwell, C., 2009. Ecological impacts of early 21st century agricultural change in Europe – A review. J. Environ. Manage. 91, 22–46. https://doi.org/10.1016/j.jenvman.2009.07.005

Stöckle, C.O., Donatelli, M., Nelson, R., 2003. CropSyst, a cropping systems simulation model. Eur. J. Agron., Modelling Cropping Systems: Science, Software and Applications 18, 289–307. https://doi.org/10.1016/S1161-0301(02)00109-0

Stoddard, F.L., Nicholas, A.H., Rubiales, D., Thomas, J., Villegas-Fernández, A.M., 2010. Integrated pest management in faba bean. Field Crops Res., Faba Beans in Sustainable Agriculture 115, 308–318. https://doi.org/10.1016/j.fcr.2009.07.002

Tribouillois, H., Dürr, C., Demilly, D., Wagner, M.-H., Justes, E., 2016. Determination of Germination Response to Temperature and Water Potential for a Wide Range of Cover Crop Species and Related Functional Groups. PLOS ONE 11, e0161185. https://doi.org/10.1371/journal.pone.0161185

Unkovich, M., 2008. Measuring plant-associated nitrogen fixation in agricultural systems. Australian Centre for International Agricultural Research, Canberra.

Wallach, D., Buis, S., Lecharpentier, P., Bourges, J., Clastre, P., Launay, M., Bergez, J.-E., Guerif, M., Soudais, J., Justes, E., 2011. A package of parameter estimation methods and implementation for the STICS crop-soil model. Environ. Model. Softw. 26, 386–394. https://doi.org/10.1016/j.envsoft.2010.09.004

Watson, C.A., Reckling, M., Preissel, S., Bachinger, J., Bergkvist, G., Kuhlman, T., Lindström, K., Nemecek, T., Topp, C.F.E., Vanhatalo, A., Zander, P., Murphy-Bokern, D., Stoddard, F.L., 2017.

870 Grain Legume Production and Use in European Agricultural Systems. Adv. Agron. 144, 235–
871 303. https://doi.org/10.1016/bs.agron.2017.03.003
872

Figures:

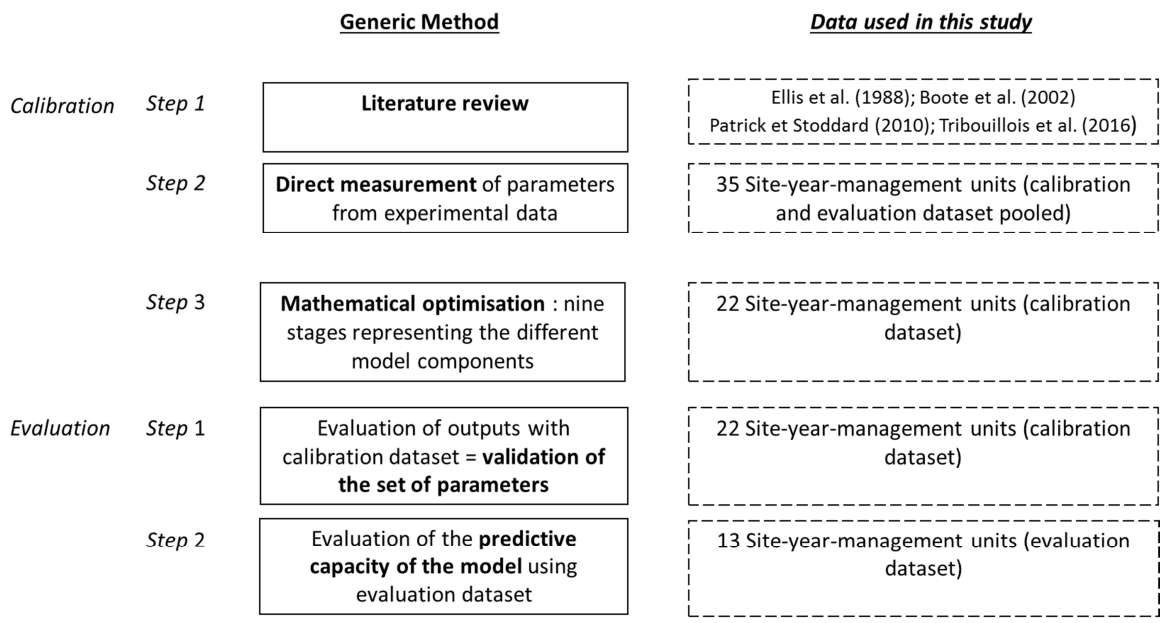

Figure 1: Summary of the generic method used for calibration and evaluation of faba bean with the STICS soil/crop model and data used for this study.

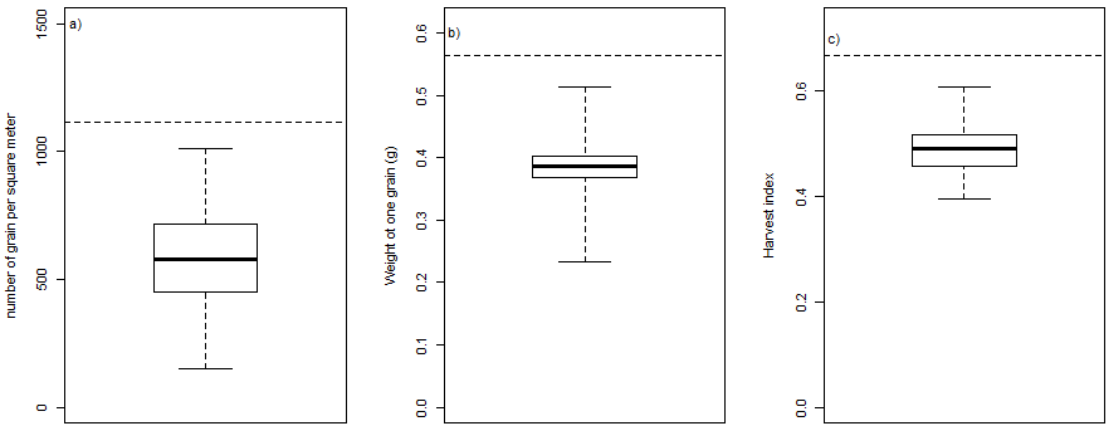

Figure 2: Boxplots of number of grain per square meter (a), weigh of one grain (b) and harvest index (c) in the 35 site-year-management units of the study. The horizontal line in the box indicates the median. The height of the box represents the interquartile range. The whiskers extend to the maximum values. The horizontal dotted line correspond to the maximum measured values with an added 10% to define potential maximum values in the *STICS* model.

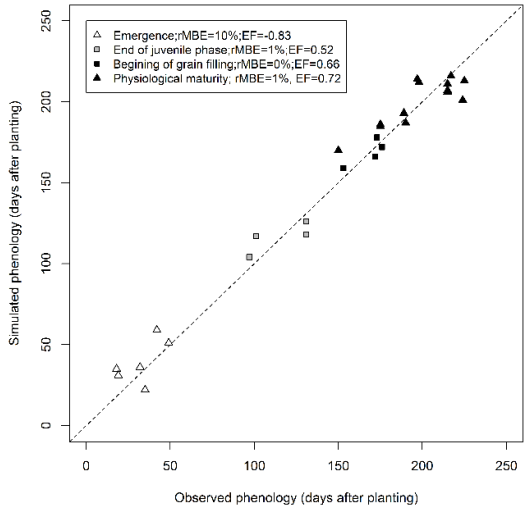

Figure 3: Comparison of observed and simulated (*STICS* model) faba bean phenology.

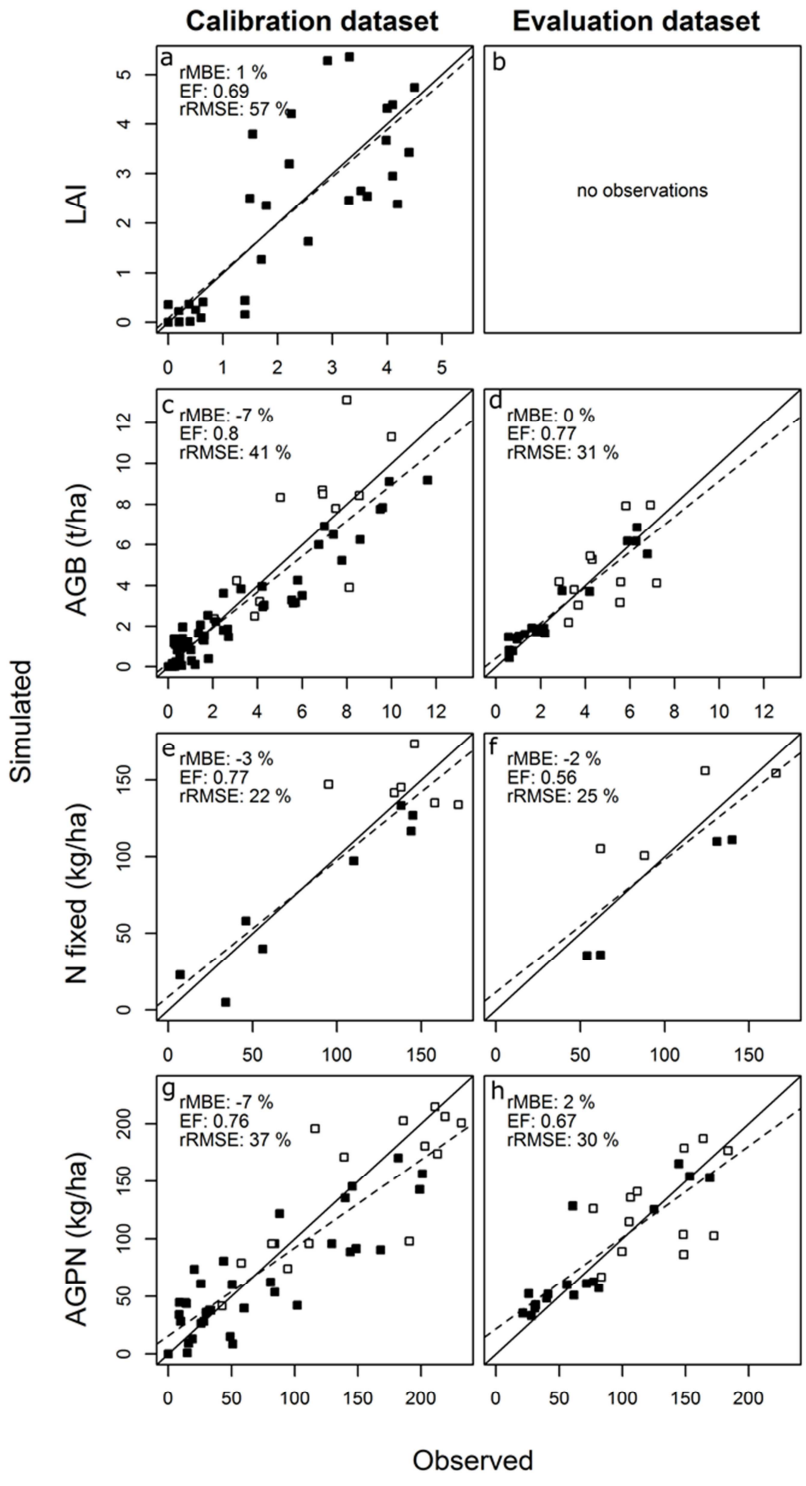

Figure 4: Comparison of observed and *STICS* simulated LAI, Above ground biomass (AGB), N_2 fixed, and Above ground plant N (AGPN) for calibration and evaluation dataset. rMBE = relative mean bias error, EF= model efficiency, rRMSE = relative Root Mean Square Error. The black line is the 1:1 line. The dotted line represent the regression of simulated against observed values. White symbols correspond to the end of growing season.

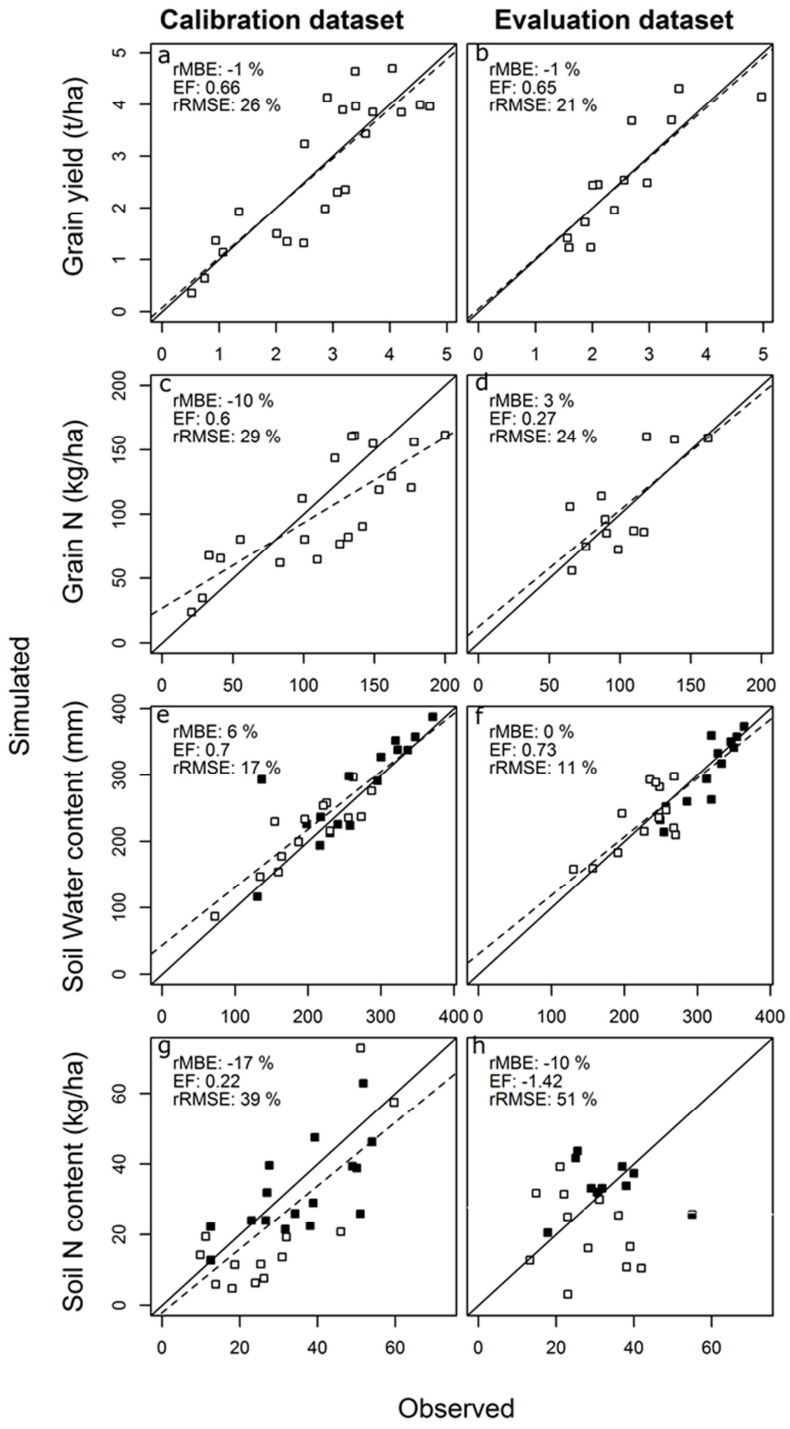

Figure 5: Comparison of observed and *STICS* simulated grain yield, grain N, soil water content, and soil mineral N content for calibration and evaluation dataset. rMBE = relative mean bias error, EF= model efficiency, rRMSE = relative Root Mean Square Error. The black line is the 1:1 line. The dotted line represent the regression of simulated against observed values (plotted when significant at 5% risk level). White symbols correspond to the end of growing season.

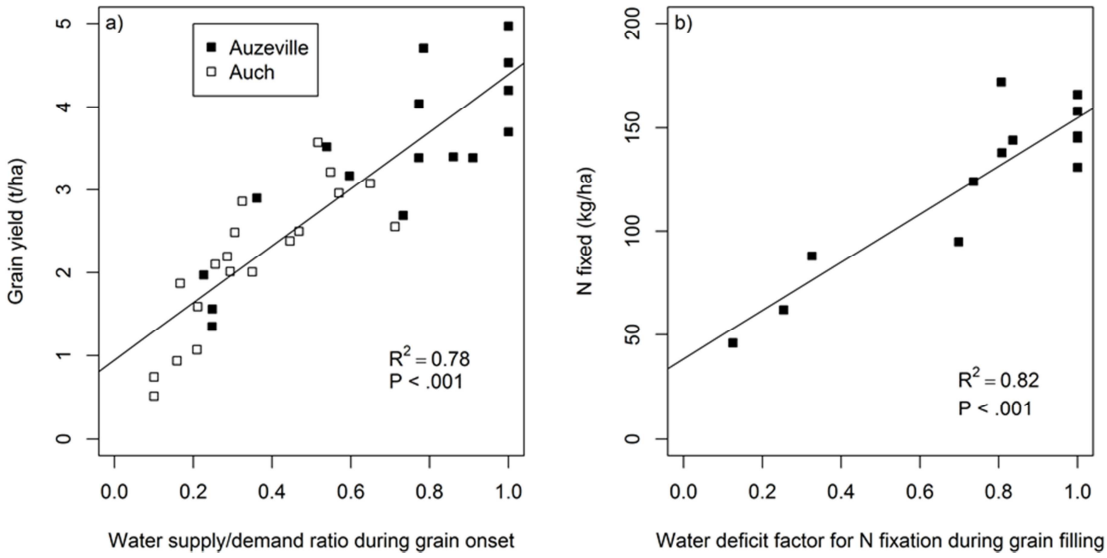

Figure 6: Correlation (a) between grain yield and average water supply/demand ratio during grain onset (over the six days before beginning of grain filling) and (b) total N_2 fixed at harvest and average water deficit factor for N_2 fixation during grain filling (over the first 20 days after beginning of grain filling). Calibration and evaluation datasets were pooled together.

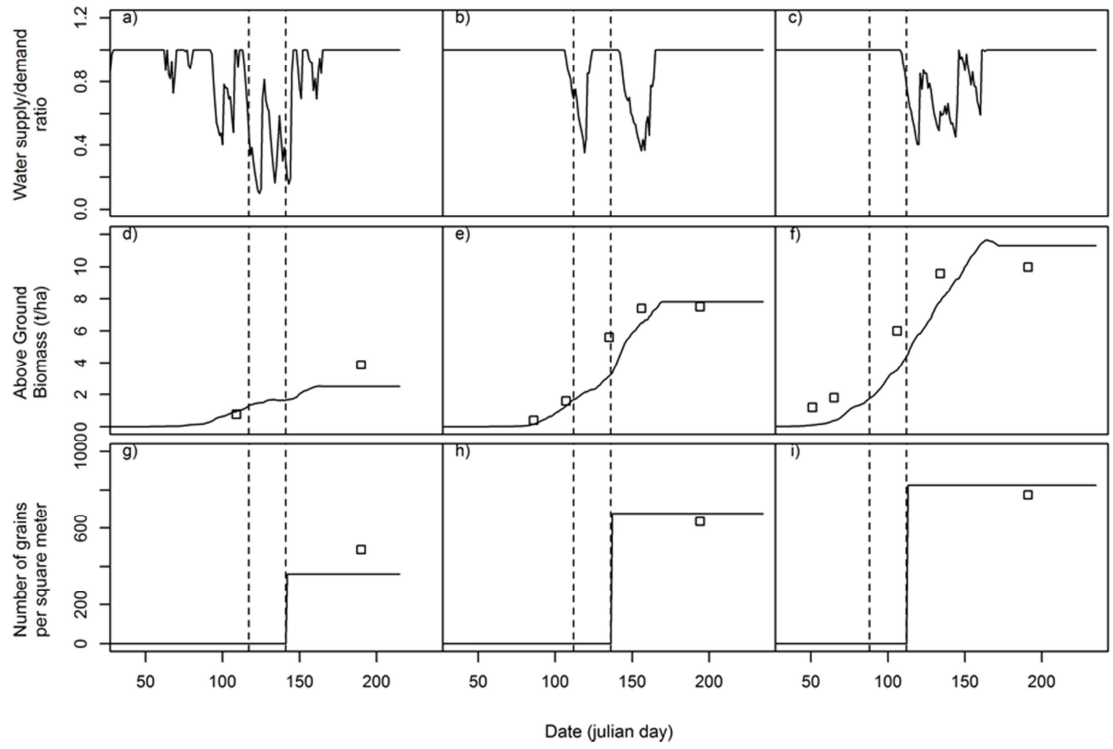

Figure 7: Example of contrasted simulated temporal dynamic (black line) of water supply/demand ratio, above ground biomass and number of grain per square meter in Auch in 2007 (a,d,g), Auzeville in 2010 (b,e,h) and Auzeville in 2007 (c,f,i) in the calibration dataset. White squares are the observations. Vertical dotted lines delimit the periods during which the correlation between average water supply/demand ratio and grain yield is maximal.

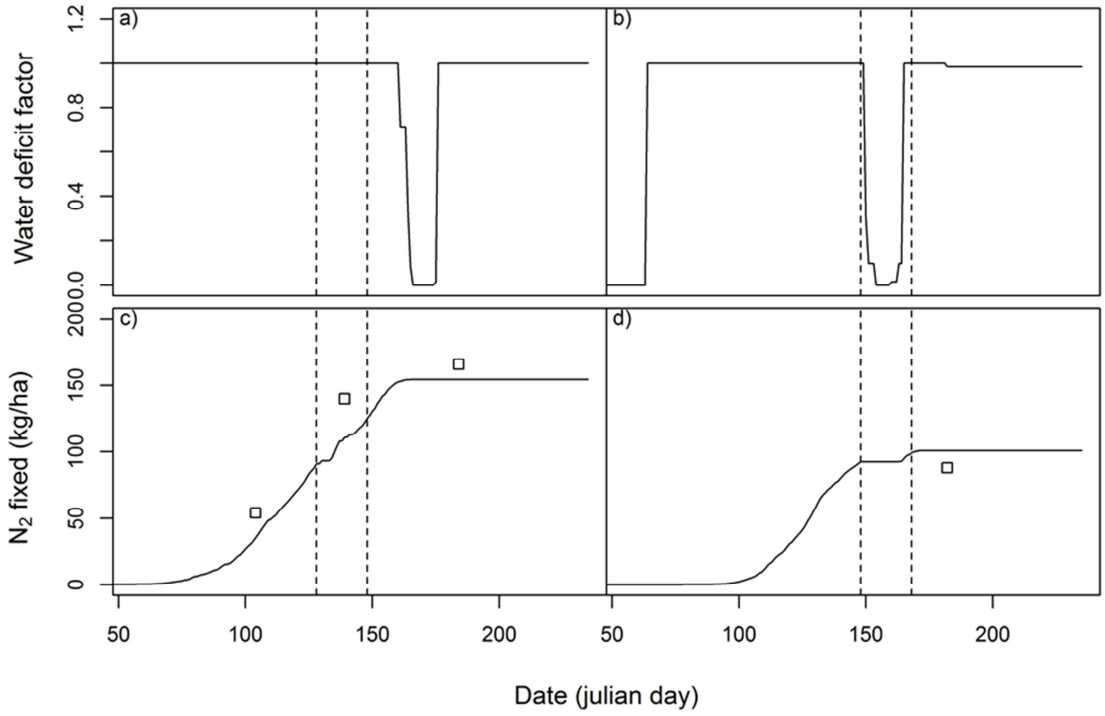

Figure 8: Example of contrasted simulated temporal dynamic (black line) of water deficit factor for N_2 fixation and N_2 fixed in Auzeville in 2014 (a, c) and 2015 (b, d) in the evaluation dataset. White squares are the observations. Vertical dotted lines delimit the periods during which the correlation between average Water deficit factor and N_2 fixation is maximal.

Tables:

Table 1: Climate and soil characteristics (averaged across growing seasons and experimental fields) in the two experimental sites (standard error in brackets)

Site	Number of growing seasons	November-July			Number of experimental fields	Clay content (0-30cm) (%)	pH (0-30cm)	Maximum rooting depth (cm)	Gravimetric moisture at field capacity* (%)	Gravimetric moisture at wilting point* (%)	Maximum available water** (mm to maximum rooting depth)
		Cumulative global solar radiation (MJ m^{-2})	Cumulative growing degree days (°C day)	Cumulative rainfall (mm)							
Auch	7	3354 (64.8)	3083 (59.1)	542 (47.2)	11	31.8 (1.46)	8.4 (0.03)	70 (4.9)	17.4 (0.45)	12.0 (0.27)	64 (4.8)
Auzeville	7	3561 (30.4)	3412 (49.1)	528 (42.8)	12	25.9 (0.97)	7.4 (0.15)	135 (4.5)	19.4 (0.43)	10.2 (0.23)	167 (8.5)

*Average across 0-30cm, 30-60cm, 60-90cm and 90-120cm soil layers.
**Soil water content at field capacity minus soil water content at wilting point.

Table 2: Description of the Site-Year-Management units in the calibration and evaluation datasets. LAI: Leaf Area Index, AGPN: above-ground plant N, AGB: above-ground biomass, GY: grain yield, GNC: grain N content, SN: Soil N content over the entire profile, SWC: soil water content over the entire profile.

			Management					Number of measurements during growing season								
Dataset	Site	Year (harvest)	Cultivar	Density (Number of plant m^{-2})	Cover crop before planting	Sowing date	Dates and amount of irrigation water	LAI	Fixed N	AGPN	AGB	GY	GNC	Root depth	SN	SWC
Calibration	Auzeville	2007	Castel	30	No	7 November	7 November - 20mm	4	1	5	5	1	1	0	2	2
			Castel	15	No	7 November	7 November - 20mm	4	1	5	5	1	1	0	2	2
		2010	Castel	30	No	19 November	0	4	2	5	5	1	1	0	2	2
			Castel	15	No	19 November	0	4	2	5	5	1	1	0	2	2
		2011	Irena	30	No	2 December	14 April; 16 May - 34;49 mm	4	4	5	5	1	1	0	2	2
			Irena	30	No	2 December	0	0	2	3	3	1	1	0	2	2
		2012	Castel	30	No	22 November	0	0	1	3	3	1	1	0	2	2
		2013	Irena	30	No	20 November	0	4	1	1	4	1	1	6	2	2
			Irena	30	No	23 November	0	0	0	0	3	1	1	0	2	2
			Irena	15	No	23 November	0	4	1	1	4	1	1	0	2	2
	Auch	2002	Castel	30	No	17 December	0	0	0	1	1	1	1	0	1	1
			Castel	30	No	17 December	0	0	0	1	1	1	1	0	1	1
		2003	Castel	30	No	20 November	0	0	0	2	2	1	1	0	2	2
		2004	Castel	30	No	25 November	0	0	0	2	2	1	1	0	2	2
			Castel	30	No	12 January	0	0	0	2	2	1	1	0	2	2
			Castel	30	No	12 January	0	0	0	2	2	1	1	0	2	2
		2005	Castel	30	No	23 November	0	0	0	2	2	1	1	0	2	2
		2007	Castel	30	No	1 December	0	0	0	2	2	1	1	0	2	2
			Castel	30	No	1 December	0	0	0	2	2	1	1	0	2	2
			Castel	30	No	1 December	0	0	0	2	2	1	1	0	2	2
		2010	Castel	30	No	11 December	0	0	0	2	2	1	1	0	2	2
			Castel	30	No	11 December	0	0	0	2	2	1	1	0	2	2
	Total						0	28	15	55	64	22	22	6	42	42
Evaluation	Auzeville	2012	Castel	30	Yes	22 November	0	0	1	3	2	1	1	0	2	2
		2013	Irena	30	Yes	23 November	0	0	0	0	3	1	0	0	2	2
		2014	Mix*	30	Yes	13 December	0	0	3	3	3	1	1	0	2	2
			Mix*	30	No	13 December	0	0	2	3	3	1	1	0	2	2
		2015	Mix*	30	Yes	13 January	0	0	1	3	3	1	1	0	2	2
			Mix*	30	No	13 January	0	0	1	3	3	1	1	0	2	2
	Auch	2003	Irena	30	No	20 November	0	0	0	2	2	1	1	0	2	2
			Irena	30	No	21 November	0	0	0	2	2	1	1	0	2	2
			Irena	30	No	22 November	0	0	0	2	2	1	1	0	2	2
		2013	Irena	30	No	17 December	0	0	0	2	2	1	1	0	2	2
			Irena	30	No	17 December	0	0	0	2	2	1	1	0	2	2
			Irena	30	No	17 December	0	0	0	2	2	1	1	0	2	2
			Irena	30	No	17 December	0	0	0	2	2	1	1	0	2	2
	Total							0	8	29	31	13	12	0	26	26

* Irena, Organdi and Diver

Table 3: Description of the nine stages undertaken for parameter optimisation: parameters optimised, minimum and maximum values, and target variable. Dd = degree (°C) day

		Parameter					Target variable		
Stage	Simulated process	Acronym	Description	Unit	Minimum	Maximum	Acronym	Description	Unit
1	Emergence	belong	parameter of coleoptile elongation curve	Dd^{-1}	0.005	0.04	ilev	date of emergence	julian day
		celong	parameter of plantlet elongation curve	-	1	10	ilev	date of emergence	julian day
2a	Crop development	sensiphot	index of photoperiod sensitivity (1=insensitive)	-	0	1	iamf	date of end of juvenile phase	julian day
		jvc	number of vernalising days	days	0	70	iamf	date of end of juvenile phase	julian day
		phobase	basal threshold controlling photoperiod slowing effect	hours	5	12	iamf	date of end of juvenile phase	julian day
		phosat	saturating threshold controlling photoperiod slowing effect	hours	6	14	iamf	date of end of juvenile phase	julian day
		stlevamf	cumulative thermal time between emergence and end of juvenile phase	Dd	100	1000	iamf	date of end of juvenile phase	julian day
2b	Crop development	stamflax	cumulative thermal time between end of juvenile phase and maximum LAI	Dd	100	1000	ilax	date when LAI is maximum	julian day
		stlevdrp	cumulative thermal time between emergence and begining of grain filling	Dd	100	1500	idrp	date of begining of grain filling	julian day
3a	Leaves	dlaimaxbrut	maximum rate of the setting up of LAI	$m^2\ plant^{-1}\ Dd^{-1}$	0.0005	0.05	lai(n)	Leaf Area index	-
		adens	interplant competition parameter	-	-2	0	lai(n)	Leaf Area index	-
		bdens	minimal density above which interplant competition starts	$plant\ m^{-2}$	1	30	lai(n)	Leaf Area index	-
		durvieF	maximal lifespan of an adult leaf	-	10	500	lai(n)	Leaf Area index	-
4	Root growth	croirac	elongation rate of the root apex	$cm\ Dd^{-1}$	0.005	0.5	zrac	Rooting depth	cm
		draclong	maximum rate of root length production per plant	$cm\ plant^{-1}\ Dd^{-1}$	1	1000	HR(1), HR(2), HR(3), HR(4)	Soil water content in layer 1,2,3,4 (%)	-
5a	Shoot growth	efcroijuv	maximum radiation use efficiency during the juvenile phase	$g\ MJ^{-1}$	1	4	masec	Above ground biomass	$t\ ha^{-1}$
		efcroirepro	maximum radiation use efficiency during the grain filling phase	$g\ MJ^{-1}$	2	5	masec	Above ground biomass	$t\ ha^{-1}$
		efcroiveg	maximum radiation use efficiency during the vegetative stage	$g\ MJ^{-1}$	2	5	masec	Above ground biomass	$t\ ha^{-1}$
5b	Shoot growth	abscission	fraction of senescent leaves falling to the soil	-	0	100	masec	Above ground biomass	$t\ ha^{-1}$
		ratiosen	fraction of senescent biomass (relative to total biomass)	-	0	1	masec	Above ground biomass	$t\ ha^{-1}$
6	Nitrogen fixation	fixmaxgr	maximal N symbiotic fixation rate per unit of grain growth rate	$kg\ t^{-1}$	0	50	Qfix	Above ground fixed plant N	$kg\ ha^{-1}$
		fixmaxveg	maximal N symbiotic fixation rate per unit of vegetative growth rate	$kg\ t^{-1}$	0	50	Qfix	Above ground fixed plant N	$kg\ ha^{-1}$
7	Nitrogen uptake	Kmabs2	affinity constant of N uptake by roots for the low uptake system	$\mu mole\ L^{-1}$	4000	40000	QNplant	Total Above ground plant N	$kg\ ha^{-1}$
		Vmax2	maximum specific N uptake rate with the high affinity transport system	$\mu mole\ cm^{-1}\ h^{-1}$	0.002	0.1	QNplant	Total Above ground plant N	$kg\ ha^{-1}$
8a	Yield formation	cgrain	slope of the relationship between grain number and growth rate	$grains\ g^{-1}\ day$	0.01	1	chargefruit	Number of filling grains	$grains\ m^{-2}$

		nbjgrain	number of days used to compute the number of viable grains	days	5	40	chargefruit	Number of filling grains	grains m^{-2}
		cgrainv0	number of grains produced when growth rate is zero	grains m^{-2}	0	15000	chargefruit	Number of filling grains	grains m^{-2}
8b	Yield formation	vitircarb	rate of increase of the C harvest index versus time	g grain.g $^{-1}$ day^{-1}	0.001	0.02	mafruit	Grain yield	t ha^{-1}
		tmaxremp	maximal temperature above which grain filling stops	°C	10	40	mafruit	Grain yield	t ha^{-1}
9	Grain N content	vitirazo	rate of increase of the N harvest index versus time	g grain g^{-1} d^{-1}	0.001	0.06	QNgrain	Grain N content	kg ha^{-1}

Table 4: Values of faba bean parameter as calibrated in the *STICS* crop model for experiments in Auch and Auzeville, France.

	Parameter			
Process	Acronym	Description	Value	Source
Emergence	tdmin	basal temperature for crop development	0	Tribouillois et al. (2016)
	belong	parameter of coleoptile elongation curve	0.0200	mathematical optimisation
	celong	parameter of plantlet elongation curve	6.20	mathematical optimisation
Crop development	sensiphot	index of photoperiod sensitivity (1=insensitive)	0.6	mathematical optimisation
	jvc	number of vernalising days	3	mathematical optimisation
	phobase	basal photoperiod controlling photoperiod slowing effect	5.7	mathematical optimisation
	phosat	saturating photoperiod controlling photoperiod slowing effect	12	mathematical optimisation
	stlevamf	cumulative thermal time between emergence and end of juvenile phase	518	mathematical optimisation
	stamflax	cumulative thermal time between end of juvenile phase and maximum LAI	700	mathematical optimisation
	stlevdrp	cumulative thermal time between emergence and begining of grain filling	1180	mathematical optimisation
Leaves	dlaimaxbrut	maximum rate of the setting up of LAI	0.0025	mathematical optimisation
	adens	interplant competition parameter	-0.50	mathematical optimisation
	bdens	minimal density above which interplant competition starts	1	mathematical optimisation
	durvieF	maximal lifespan of an adult leaf	220	mathematical optimisation
Root growth	croirac	elongation rate of the root apex	0.07	mathematical optimisation
	draclong	maximum rate of root length production per plant	810	mathematical optimisation
Shoot growth	efcroijuv	maximum radiation use efficiency during the juvenile phase	1	mathematical optimisation
	efcroirepro	maximum radiation use efficiency during the grain filling phase	3.5	mathematical optimisation
	efcroiveg	maximum radiation use efficiency during the vegetative stage	2.3	mathematical optimisation
	abscission	fraction of senescent leaves falling to the soil	1	mathematical optimisation
	ratiosen	fraction of senescent biomass (relative to total biomass)	0.75	mathematical optimisation
	temin	basal temperature for photosyntesis	0	Tribouillois et al. (2016)
	teopt	optimal temperature for photosynthesis	24	Tribouillois et al. (2016)
	temax	maximal temperature for photosynthesis	34	Tribouillois et al. (2016)
Nitrogen fixation	fixmaxgr	maximal N symbiotic fixation rate per unit of grain growth rate	17	mathematical optimisation
	fixmaxveg	maximal N symbiotic fixation rate per unit of vegetative growth rate	27	mathematical optimisation
	tempnod1,2,3,4	cardinal temperatures driving N_2 fixation	0,16,25,40	Boote et al. (2002)
Nitrogen uptake	Kmabs2	affinity constant of N uptake by roots for the low uptake system	33300	mathematical optimisation
	Vmax2	maximum specific N uptake rate with the high affinity transport system	0.16	mathematical optimisation
Yield formation	cgrain	slope of the relationship between grain number and growth rate	0.0475	mathematical optimisation
	nbjgrain	number of days used to compute the number of viable grains	9	mathematical optimisation
	cgrainv0	number of grains produced when growth rate is zero	0.172	mathematical optimisation
Yield formation	vitircarb	rate of increase of the C harvest index vs time	0.04	mathematical optimisation
	tmaxremp	maximal temperature above which grain filling stops	33	mathematical optimisation
	nbgrmin	minimum number of grains	360	Measurement

	nbgrmax	maximum number of grains	1120	Measurement
	pgrainmaxi	maximum weight of one grain	0.57	Measurement
	irmax	maximum harvest index	0.6	Measurement
Grain N content	vitirazo	rate of increase of the N harvest index versus time	0.056	mathematical optimisation